

Energy calibration of the $^{40}\text{Ca} + ^{40}\text{Ca}$ data taken on the NIMROD-ISiS array

K. Schmidt, C. Bottosso, J. B. Natowitz, K. Hagel, R. Wada, M. Huang, A. Bonasera, M. Barbui, M. Rodrigues, G. Liu,¹ G. Viesti,² S. Moretto,² G. Prete,³ S. Pesente,² D. Fabris,² Y. El Masri,⁴ T. Keutgen,⁴ S. Kowalski,⁵ and A. Kumar⁶

¹*Shanghai Institute of Applied Physics, Shanghai, China*

²*Dipartimento di Fisica dell'Universita di Padova and INFN Sezione di Padova, Italy*

³*INFN Laboratori Nazionali di Legnaro, Italy*

⁴*Universit'e Catholique de Louvain, Louvain-la-Neuve, Belgium,*

⁵*Institute of Physics, Silesia University, Katowice, Poland*

⁶*Nuclear Physics Laboratory, Department of Physics, Banaras Hindu University, Varanasi, India*

The ability to isolate low density matter in near Fermi Energy collisions and the high degree of alpha clustering which is observed suggest that we search for evidence of Bose Condensates which are predicted to occur in the density and temperature range which we explore in near Fermi energy collisions [1-3]. We have initiated a search for evidence of Bose Condensates using the NIMROD array. Our first experiments, carried out at the end of 2008 employed 10, 25, 35 MeV/u beams of ^{40}Ca and ^{28}Si incident on ^{40}Ca , ^{28}Si , ^{12}C and ^{180}Ta targets. The first three targets allow an exploration of collisions of alpha conjugate nuclei. In the ^{180}Ta case the projectile excitation and decay is of primary interest. Before a more sophisticated analysis is performed the mass, charge and energy of detected fragments must be determined.

The identification in mass and charge [4] for all systems is now complete. The energy calibration consists of several steps and the first one is the super-telescope calibration. The Si₁-Si₂ silicon detectors are "self-calibrating" as we employ range energy tables to established from the punch through points of

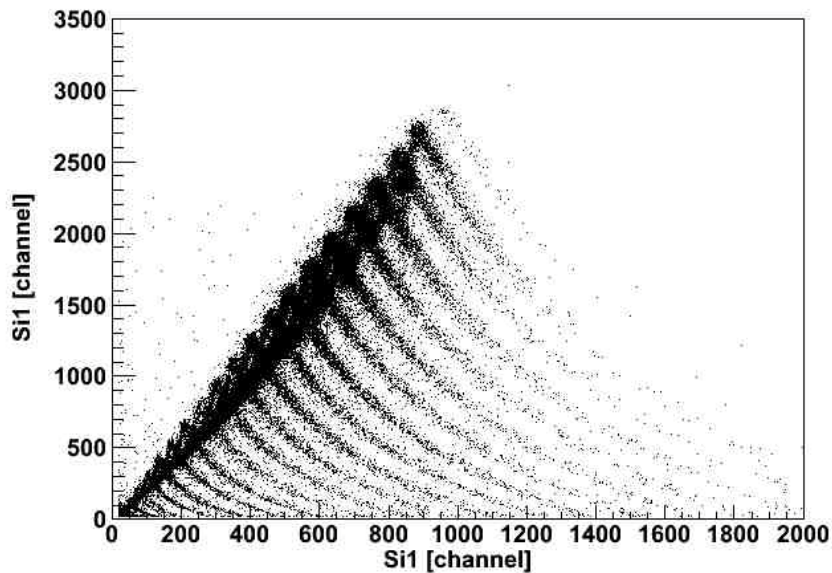


FIG. 1. Si1 signal vs Si2 signal.

various identified species. In Fig. 1 the signals from both silicon detectors of a typical super-telescope are plotted. We note that the position of the punch through points can be very precisely determined.

Once the super-telescope calibrations are established, we calculate the energy deposited in CsI scintillators behind them. Relating the deposited energy to channel numbers allows us to find the calibration parameters of light particles stopped in CsI scintillator. The green low energy points in Fig. 2. show the energy deposited by α particles in the CsI versus the light output of the Slow signal. The other green, black and red points show the elastic scattering points of p, d, and α particles on Ca target at energies 25MeV/A, 30MeV/A and 55MeV/A obtained in a later calibration run. We applied the global fit to the spectra, using a formula based on the Tabacaru's prescription [5]:

$$L = a_5 + a_0 \left(E \left(1 - \frac{a_1 AZ^2}{E} \ln \left(1 + \frac{E}{a_1 AZ^2} \right) \right) c_1 a_1 AZ^2 \ln \left(\frac{E + a_1 AZ^2}{a_1 a_2 AZ^2} \right) \right) + M;$$

$$c_0 = \frac{a_3}{1 + e^{\frac{a_4}{a_2}}};$$

$$c_1 = \frac{a_3}{1 + e^{-\frac{(E-a_2)}{a_4}}};$$

$$M = -a_0 c_0 a_1 AZ^2 \ln \left(\frac{a_1 AZ^2}{a_1 AZ^2 + a_2} \right).$$

The solid black, red and green lines in Fig. 2. correspond to the modified Tabacaru function for p, d, and α , respectively. The Tabacaru parameters allow us to transform the light output from the CsI to energy in the scintillator using one function that depends on light output, charge and mass.

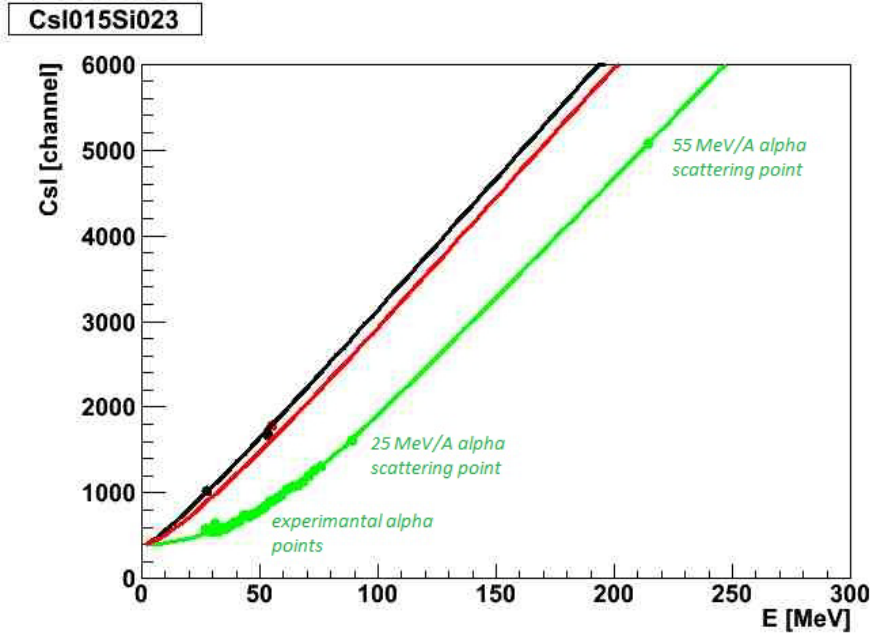


FIG. 2. The energy deposited in CsI detectors by p (black points), d (red points) and α particles (green points) versus CsI slow signal. The solid black, red and green lines correspond to the Tabacaru function for p, d, and α , respectively.

To determine the energies of light particles detected in the other detectors in the same NIMROD ring, we used the energy spectra of the super-telescopes as a reference spectra and applied a χ^2 based fitting procedure to determine calibration parameters. In Fig. 3 we show the comparison between the reference energy spectra (black lines) and calibrated spectra (red lines) for protons (left) and alpha particles (right) stopped in the detectors placed in the second Ring of NIMROD. The other rings showed similar results.

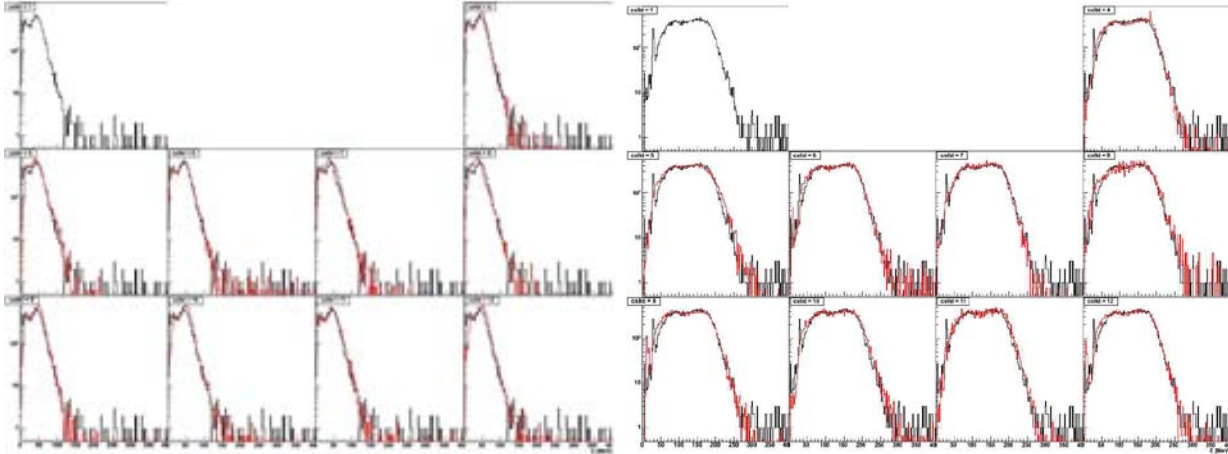


FIG. 3. The comparison between the reference energy spectra (black lines) and calibrated spectra (red lines) for protons (left) and alpha particles (right) stopped in the detectors placed in the second Ring of NIMROD array.

The calibration procedure for heavier fragments is in progress. To determine the energy of the heavier fragments we use the energy loss in the silicon detectors to determine the initial energy. The procedure for the heavy fragment calibration is to use the spectra from the super-telescopes as reference spectra and perform the χ^2 minimalisation to establish the calibration of the other silicon detectors. As soon as the calibration of the heavier fragments is completed, we will begin the advanced analysis.

- [1] Y. Funaki *et al.*, Phys. Rev. C **80**, 064326 (2009).
- [2] G. Roepke *et al.*, Phys. Rev. Lett. **80**, 3177(1998).
- [3] T. Sogo *et al.*, Phys. Rev. C **81**, 064310 (2010).
- [4] C. Bottosso *et al.*, *Progress in Research*, Cyclotron Institute, Texas A&M University (2008-2009), p. II-7, http://cyclotron.tamu.edu/2009_20Progress_20Report/2_20Heavy_20Ion_20Reactions/II_7_calibration_20of_20the_2040car.pdf
- [5] M. Parlog *et al.*, Nucl. Instrum. Methods Phys. Res. **A482**, 693 (2002).